

RESEARCH ON BASIC STRENGTH PERFORMANCE OF TITANIUM ALLOY LAMINATED STRUCTURE

Tianjiao Zhao¹, Zhinan Zhang¹, Jipeng Zhang², Haichao Cui³, Yuan Zhao⁴, Bintuan Wang^{1,*}

¹ The First Aircraft Institute of AVIC, Xi'an, Shaanxi Province, China

² College of Traffic and Vehicle Engineering, Shandong Institute of Technology, Zibo, Shandong Province, China

³ Composite Center of AVIC Manufacturing Technology Research Institute, Beijing, China

⁴ College of Engineering, Zhejiang Normal University, Jinhua, Zhejiang Province, China

Email:313533653@qq.com

Abstract: This article conducts theoretical analysis and experimental research on the basic mechanical properties of titanium alloy laminated structures, and analyzes the influence of design parameters such as metal volume fraction, layering method and angle on the static tensile mechanical properties. The test results verified the validity of the calculation model for the static behavior of titanium alloy laminated structure under static tensile, shear and bending conditions, and obtained the static tensile strength, shear strength and bending strength of 0° and 45° layering angle.

Keywords: Titanium alloy laminated structure, Static behavior, Failure analysis, Finite element simulation

INTRODUCTION

The Titanium alloy Laminated structure, also known as TiGr (Titanium/Graphite Hybrid Laminates), is a kind of hybrid composite material formed by alternated layering of titanium alloy and reinforced graphite fiber, as shown in Figure 1. It not only has excellent fatigue and damage tolerance, flame retardancy and impact resistance, but also has low density and high specific strength. Compared with Glass fiber metal laminates (GLARE), TiGr using titanium alloy and carbon fiber, can improve the strength, modulus and fatigue resistance of laminate.

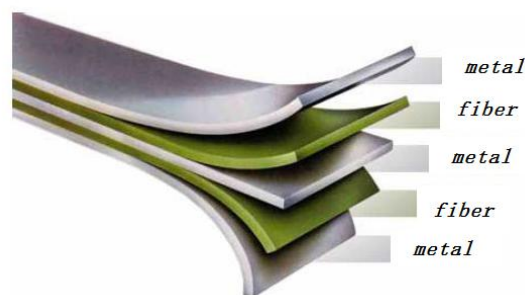


Figure 1: Schematic diagram of fiber metal laminates.

TiGr combines the isotropic properties of metal materials and the anisotropic properties of composite materials, presenting a heterogeneous state in the thickness direction. There are significant differences in stress and load transfer compared to composite materials. The strength calculation method of traditional composite laminated structure is not suitable, and a reasonable structural design method is beneficial for improving the safety of material applications, Establishing a new mechanical evaluation model for hybrid materials is of great significance for structural design.

STRENGTH FAILURE THEORY OF TIGR

TiGr has complex failure characteristics, including fiber-matrix debonding, splitting, fiber fracture, matrix cracking, matrix metal delamination, etc. It is found that the layering direction affects the failure behavior of TiGr. Due to the bridging effect of fibers, fibers that are consistent with the shear stress can transfer the stress better. For TiGr with different type, the stiffness will bring the change of load distribution, but also have a certain impact on the failure mode; In addition, the change of type will bring the change of metal volume fraction, so as to affect the distribution of stress, which is also an important factor affecting the failure behaviour[1]. Due to the complexity of material composition and structure, the existing classical laminates theory can not be directly used to predict the properties of titanium alloy laminates.

At present, the performance prediction of TiGr is mainly divided into analytical method and finite element method. In the analytical method, the metal volume fraction theory can simply predict the ultimate strength of TiGr under plane stress, but because the residual stress of each component and the interfacial stratification are not considered, the predicted result is larger than the actual value. At the same time, considering the difference between the elastic-plastic stress-strain relation of metal layer and the constitutive relation of fiber-reinforced resin composite, the failure strain and failure strength of TiGr can be obtained by extending the classical laminates theory to the stiffness matrix of metal-containing laminates[2], and the influence of different fiber angles on the tensile modulus and strength can be predicted more accurately.

On the basis of experiments, the static strength properties of TiGr are further studied by finite element method, including tensile, shear and bending conditions, and the influence of structural parameters on mechanical properties is analyzed. the finite element and theoretical analysis model established here can provide theoretical guidance and prediction method for the mechanical property evaluation of TiGr, it also can reveal the damage mechanism based on the experiment.

BASIC MECHANICAL PERFORMANCE TEST

Naming Rules

There are five types of TiGr in this paper: Ti/0/0/Ti, Ti/0/0/Ti/0/0/Ti, Ti/0/0/Ti/0/0/Ti, Ti+45/-45/Ti and Ti/+45/-45/Ti/-45/45/Ti. The five structures mentioned above are named with reference to the naming rule of Glare, as shown in Table 1.

Table 1: Naming rule of TiGr.

NO.	Type of structure	Naming
1	Ti/0/0/Ti	TiGr2A21
2	Ti/0/0/Ti/0/0/Ti	TiGr2A32
3	Ti/0/0/Ti/0/0/Ti/0/0/Ti	TiGr2A43
4	Ti+45/-45/Ti	TiGr6A21
5	Ti/+45/-45/Ti/-45/45/Ti	TiGr6A32

Test Piece Form

There are three types of test pieces: tensile test pieces, in-plane shear test pieces and three-point bending test pieces. The selected titanium alloy brand is TC4, its chemical composition is Ti-6Al-4V, and its thickness is 0.3mm. The fiber layer is carbon fiber CCF300, the thickness of prepreg monolayer is 0.125mm, and the thickness of adhesive film layer is 0.15mm. The form of test piece is shown in Figure 2.

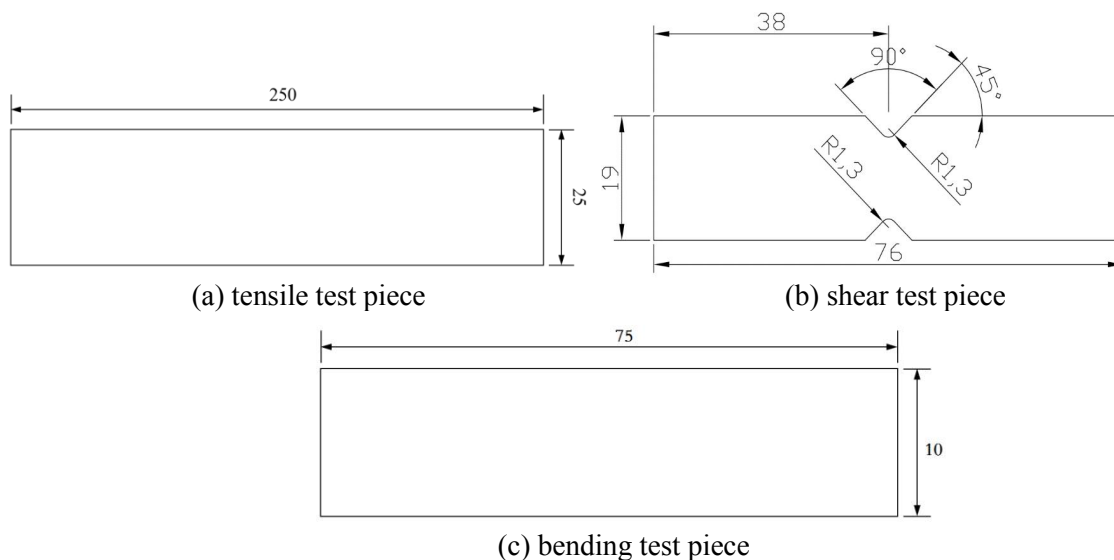


Figure 2: Schematic diagram of the static test pieces.

TEST RESULTS

Tensile Test

The morphology of two types of TiGr after tensile failure is shown in Figure 3. TiGr2A21 has transverse fracture failure, and the metal at the fracture site has a small necking phenomenon. TiGr6A21 exhibits shear failure in 45° direction without necking phenomenon.

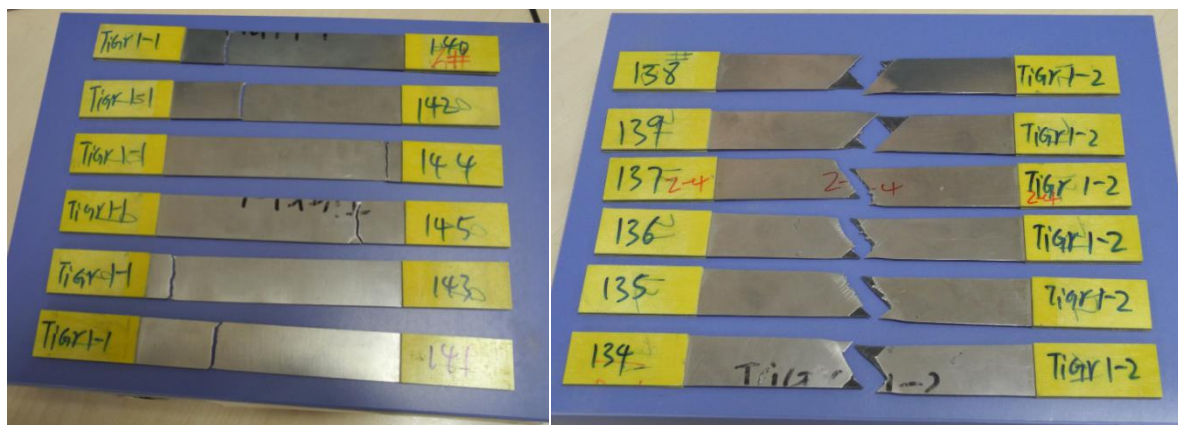
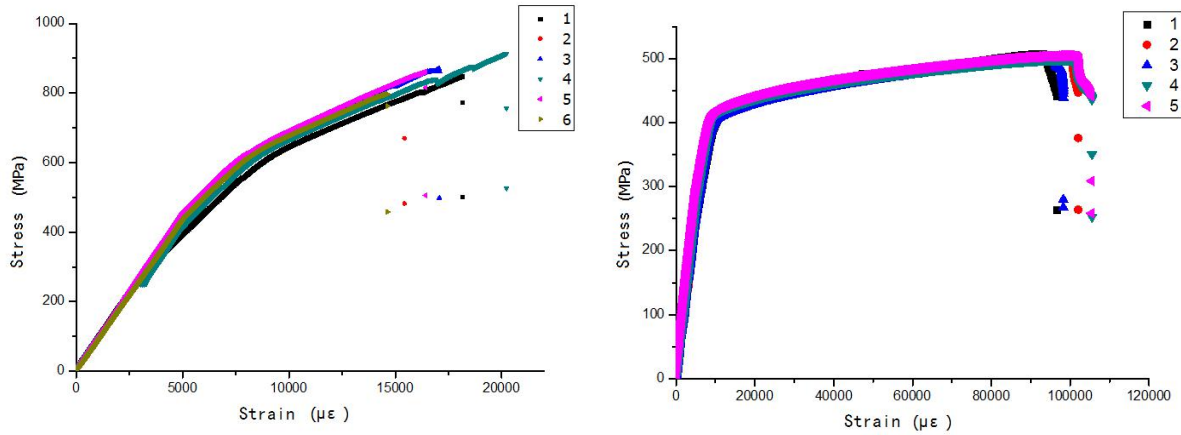


Figure 3: Morphology of TiGr2A21 and TiGr6A21 after failure.



(a) TiGr2A21 test piece

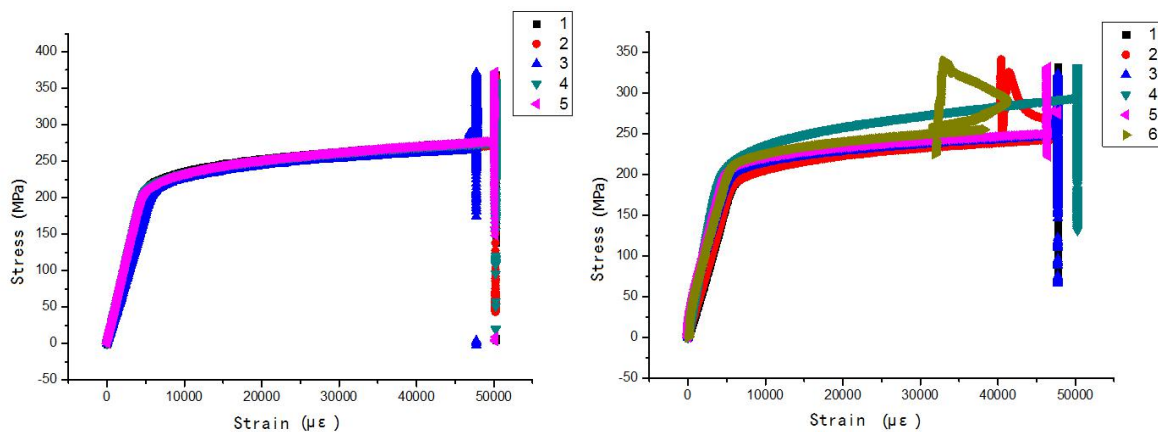
(b) TiGr6A21 test piece

Figure 4: Stress-strain curves of TiGr2A21 and TiGr6A21.

The tensile stress-strain curves of the two types of TiGr are shown in Figure 4. It can be seen from the stress variation trend that: 1) TiGr can be divided into three stages during the tensile process, the first stage is the elastic stage, the second stage is the yield stage, which is caused by the yield phenomenon of the metal, and the third stage is the linear tensile failure stage. 2) The tensile failure process presents a yield state. Due to the existence of 0° fiber layer, TiGr2A21 mainly relies on the composite material layer for load-bearing, and the yield process is more gentle after the mixture of metal and composite materials, while the TiGr6A21 with 45° fiber layer shows stronger metal characteristics. The inflection point of yield is more obvious.

In-plane Shear Test

Due to the existence of the metal layer, the surface of TiGr has a large deformation and local convex, and the shear failure occurs in the carbon fiber composite layer. The stress-strain curves of the two types of structures are shown in Figure 5. The initial stress increases linearly with the increase of strain, and after the yield inflection point, the stress slows down with the increase of strain.



(a) TiGr2A32 test piece

(b) TiGr2A43 test piece

Figure 5: Stress-strain curves of TiGr2A32 and TiGr2A43.

Bending Test

The bending properties of TiGr2A32, TiGr6A32 and TiGr2A43 are tested. The testing process is shown in Figure 6. It shows a large deflection, and the bending strength of the three types of materials is shown in Table 2.

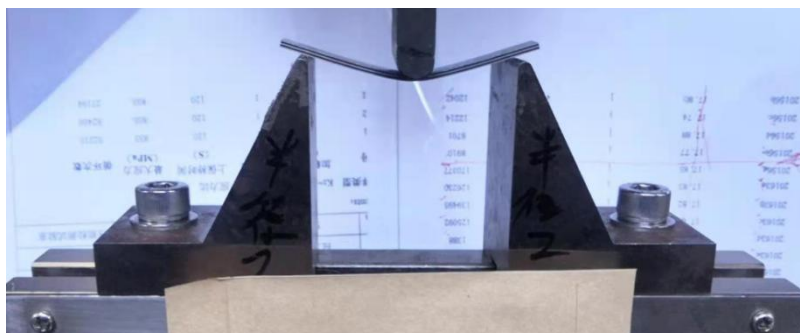


Figure 6: Bending test process.

Table 2: Bending strength.

NO.	Type	Bending strength	Variable coefficient
1	TiGr2A32	1325MPa	8.46%
2	TiGr6A32	915MPa	5.43%
3	TiGr2A43	1247MPa	8.79%

ESTABLISHMENT OF FINITE ELEMENT MODEL

Material

When establishing the finite element model of TiGr in this project, titanium alloy layer is defined as an isotropic elastic-plastic material, and its plastic deformation behavior is described using the Mises yield criterion. its basic properties are shown in Table 3. The plastic deformation behavior of titanium alloy in the finite element model is described using a true stress-strain relationship.

Table 3: Properties of TC4.

Parameter name	Numerical value
Elastic modulus E	95.83 GPa
Poisson's ratio ν	0.33
Ludwik hardening curve	$\sigma = 1238\varepsilon^{0.04}$
Ultimate strength	1099.28 MPa
Thermal expansion coefficient	$8.6 \text{ E-}6^{\circ}\text{C}^{-1}$
Density	4.51 g/cm^3

CCF300/5228A carbon fiber/epoxy composite layer (hereinafter referred to as "CFRP") is defined as orthotropic material, and its basic parameters are shown in Table 4. In finite element analysis, Hashin failure criterion is used to identify the damage generation, which considers four failure modes: fiber tensile failure, fiber compression failure, matrix tensile failure and matrix compression failure respectively[3].

Table 4: Properties of CCF300/5228A composites.

Parameter name	Value	Parameter name	Value
Elastic modulus in direction 1	131 GPa	Tensile strength in direction 2	69.4MPa
Elastic modulus in direction 2	8.85GPa	Compression strength in direction 2	223 MPa
In-plane shear modulus G	4.07 GPa	In-plane shear strength S	157 MPa
Poisson's ratio ν	0.31	Thermal expansion coefficient α_{11}	0.06E-6 °C ⁻¹
Tensile strength in direction 1	1589 MPa	Thermal expansion coefficient α_{12}	26.1E-6 °C ⁻¹
Compression strength in direction 1	1243 MPa	Density	1.55g/cm ³

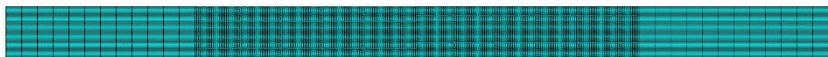
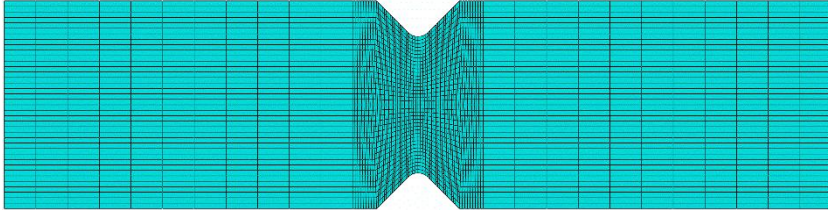
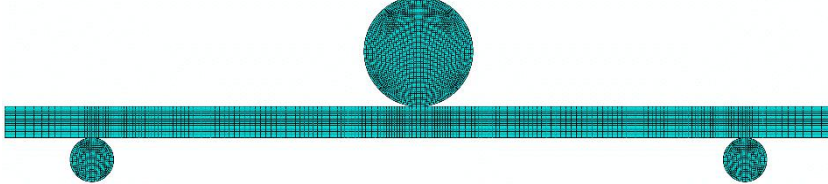
In order to accurately simulate the interface damage behavior between titanium alloy and CFRP, the cohesive model is used to define the adhesive layer in the finite element model. Because the interface damage usually occurs under the joint action of the traction force in the normal direction and the two shear directions, the secondary nominal stress criterion is used to identify the appearance of the damage.

Modeling Methods

Based on the above material models, finite element models of different types of TiGr under stretching, shearing and bending conditions are established in this paper. The geometric dimensions of the finite element models under each working condition are determined by referring to the actual test piece, as shown in Table 5.

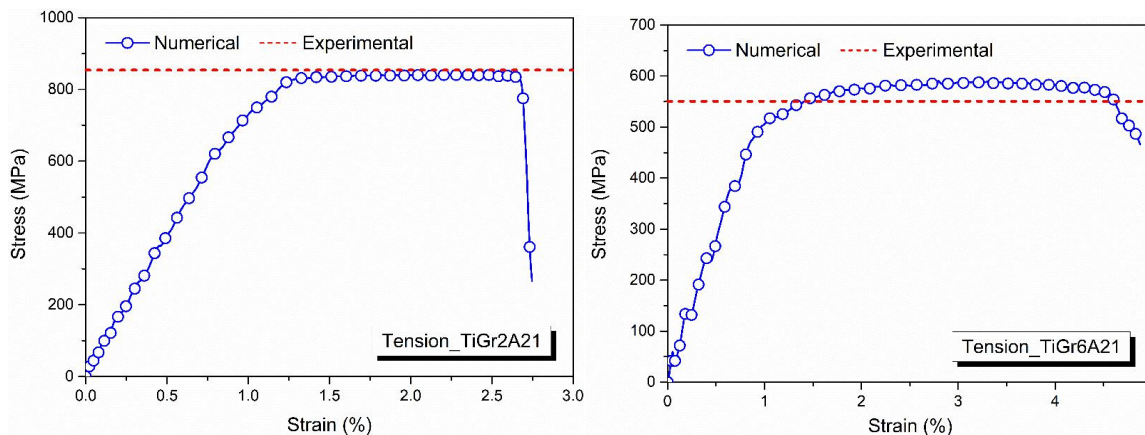
Titanium alloy, CFRP and adhesive film are discretized by 8-node hexahedral linear reduced integral element (C3D8R), 8-node quadrilateral linear reduced integral continuous shell element (SC8R) and 8-node cohesive element (COH3D8), respectively[4]. The cohesive element is connected to adjacent hexahedral and shell elements in a common node manner, and mesh refinement has been carried out on stress concentration areas to ensure the convergence and accuracy of the calculation. In order to consider the influence of thermal residual stress caused by the mismatch of thermal expansion coefficient between titanium alloy layer and CFRP layer[5], a predefined field of cooling (from curing temperature to room temperature) is defined in the model.

Table 5: Finite element model for static strength analysis.

Type	Models
Stretch	
shear	
Bending	

Analysis of Tensile Strength Calculation Results

Figure 7 shows the calculated results of the tensile stress-strain curves of TiGr2A21 and TiGr6A21, and Table 6 shows the experimental and theoretical ultimate strength values and relative errors of four types of TiGr, so as to verify the validity of the established model.



(a) tensile stress-strain curve of TiGr2A21 (b) tensile stress-strain curve of TiGr6A21

Figure 7: Tensile stress-strain curve.

Table 6: Tensile strength of TiGr.

Type of structure	Experiment (MPa)	Simulation (MPa)	Relative Error (%)
TiGr2A21	853.7	841.48	1.43
TiGr 2A32	814.5	811.76	0.34
TiGr 6A21	550.5	590.73	7.31
TiGr 6A32	502.3	519.36	3.40

It can be seen from Figure 7 and Table 6 that the established finite element model can accurately predict the tensile properties of TiGr with different types. It should be noted that this TiGr contains an epoxy adhesive film with a thickness of 0.15mm between each titanium alloy and CFRP, resulting in a higher volume fraction of the adhesive film in the structure. Due to the low modulus of the adhesive film, failure will occur in the loading process and lead to stiffness reduction. Therefore, although the volume fraction of CFRP in the 3/2 structure is higher than that in the 2/1 structure, the volume fraction of the adhesive film in the structure is also higher. The reduction of the overall stiffness of the laminated structure caused by the failure of the adhesive film is one of the main reasons affecting its bearing capacity.

Figure 8 shows the comparison of damage modes of each single layer after tensile failure of four structures, including equivalent plastic deformation of titanium alloy, tensile damage of fiber and matrix, and adhesive film failure at the interface. As can be seen from the figure, the change of the number of layers will not significantly affect the failure mechanism of the laminated structure, and the difference between the ultimate strength is small. However, When laying Angle is different, the damage mode of each single layer changes obviously. Specifically, the CFRP layer in TiGr2A laminate shows typical fiber tensile failure, and the matrix tensile failure is concentrated around the fiber damage, indicating that the fiber tensile failure plays an obvious role in failure control. While for TiGr6A laminates, it shows that when CFRP is laid along the 45° direction, the internal matrix damage plays an important role in failure control.

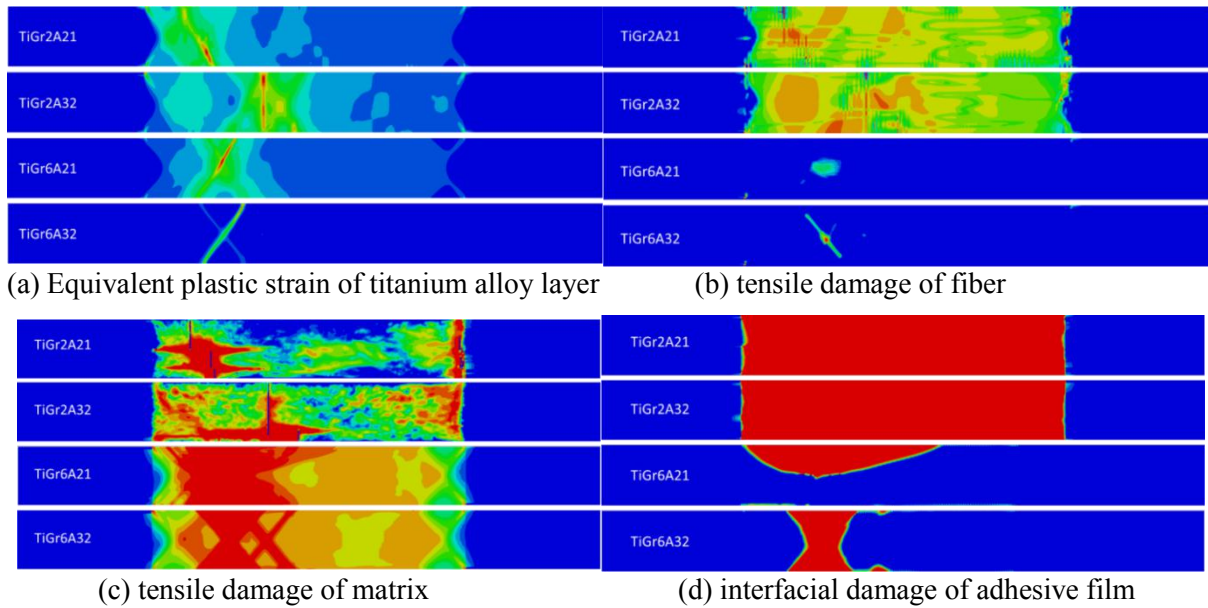


Figure 8: Analysis of tensile failure modes of TiGr2A21, TiGr2A32, TiGr6A21, and TiGr6A32.

Figure 9 shows the variation rules of tensile strength and deflection sensitivity of TiGr21 and TiGr 32 under different laying angles of fiber layer.

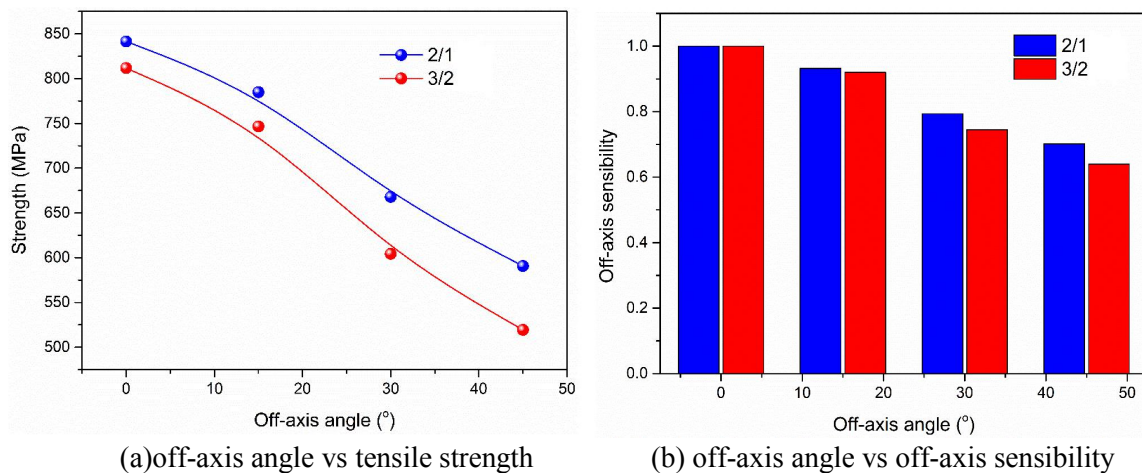
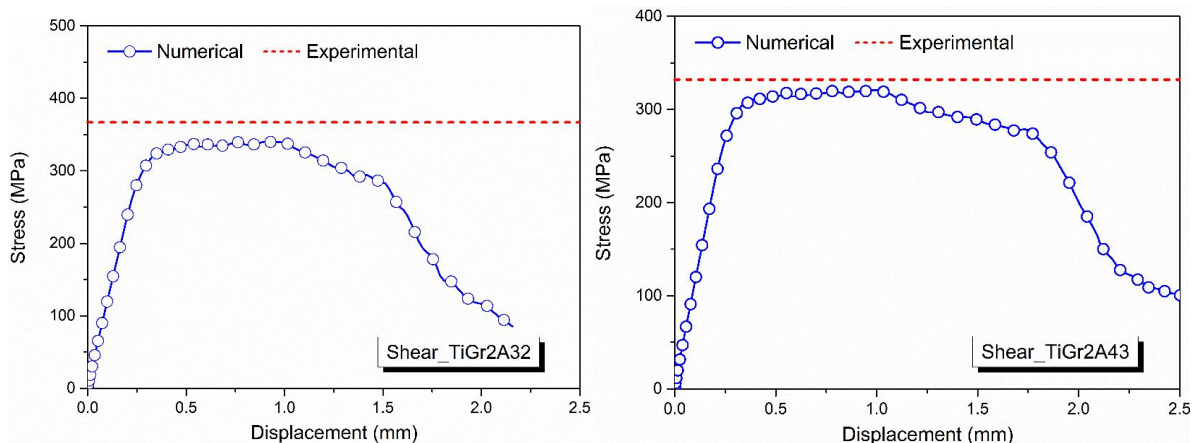


Figure 9: Influence of fiber laying Angle.

As can be seen from the figure, the strength of TiGr21 is higher than that of TiGr32, which is mainly due to the high content of adhesive film in TiGr32, and the stiffness reduction caused by the failure of adhesive film in the loading process is more serious. In addition, with the increase of the laying angle, the strength of the two types of TiGr decreased significantly. When the angle is 15°, the influence of off-axis angle is small, but when the angle is 30° and 45°, the influence of off-axis angle is larger. As can be seen from the figure, whether TiGr21 or TiGr32, when the fiber laying angle increases, its strength retention can reach more than 60%.

Analysis of Shear strength Calculation Results

Figure 10 shows the shear stress-displacement curves of TiGr2A32 and TiGr2A43, and Table 7 shows the relative error of shear strength of the two structures.



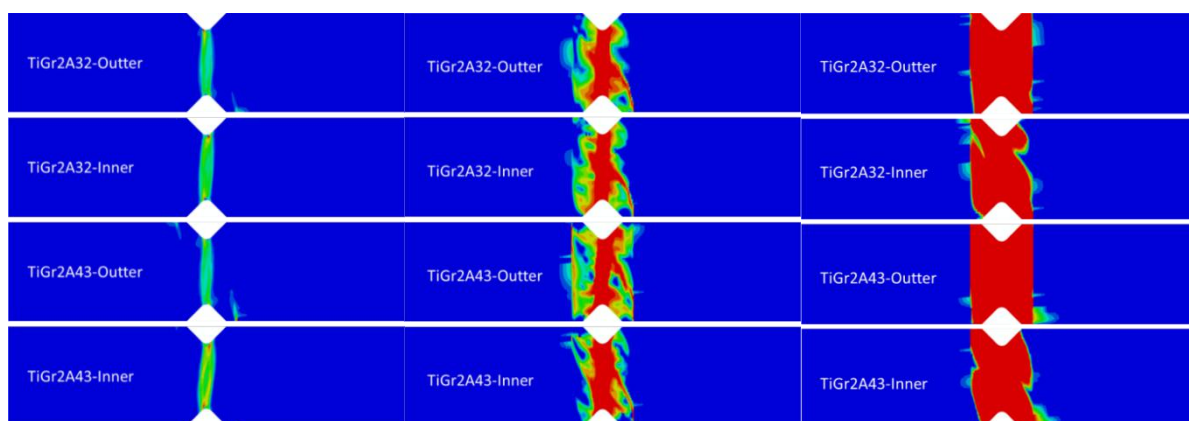
(a)TiGr2A32 stress-displacement curve (b)TiGr2A43 stress-displacement curve
Figure 10: Shear stress-displacement curve.

Table 7 Shear strength of TiGr.

Type of structure	Experiment (MPa)	Simulation (MPa)	Relative Error (%)
TiGr2A32	367	340.36	7.26
TiGr2A43	332	320.88	3.35

As can be seen from Figure 10 and Table 7, the established shear finite element model of TiGr can accurately predict its shear strength. Similarly, due to the high content of adhesive film in TiGr2A43, its shear strength is slightly lower than that of TiGr2A32, but the difference is not obvious.

Figure 11 shows the equivalent plastic deformation of the internal titanium alloy layer, the shear damage nephogram of CFRP layer and the damage nephogram of the titanium alloy -CFRP interfacial adhesive film after the shear failure respectively. As can be seen from the figure, there is no significant difference in damage modes between TiGr2A32 and TiGr2A43, including no obvious difference in damage modes between the same component at different locations. In conclusion, slightly changing the ratio of titanium alloy layer to CFRP layer does not affect its mechanical response (such as ultimate shear strength) and damage mechanism.

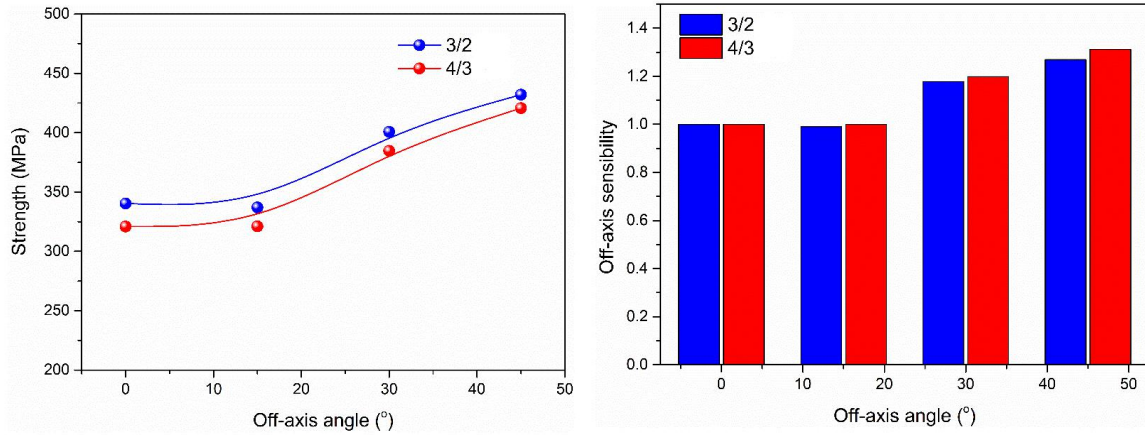


(a) Equivalent plastic strain of titanium alloy layer (b) shear damage mode of fiber layer
(c) damage mode of interfacial adhesive film

Figure 11: Analysis of shear failure modes of TiGr2A32 and TiGr2A43.

Figure 12 shows the variation of shear strength and shear off-axis sensitivity of TiGr2A32 and TiGr2A43 at different fiber laying angles. As can be seen from the figure, the shear strength of

TiGr2A32 is higher than that of TiGr2A43 under any fiber laying mode, which is related not only to the low content of adhesive film in TiGr2A32, but also to the high content of titanium alloy in it (the shear strength of titanium alloy is better than CFRP). When the fiber laying angle is 0° and 15°, the shear strength changes little, and when the laying angle increases to 30° and 45°, the shear strength increases significantly, which is mainly because the bearing ratio of the fiber layer sheared along the fiber direction increases after the laying angle increases.

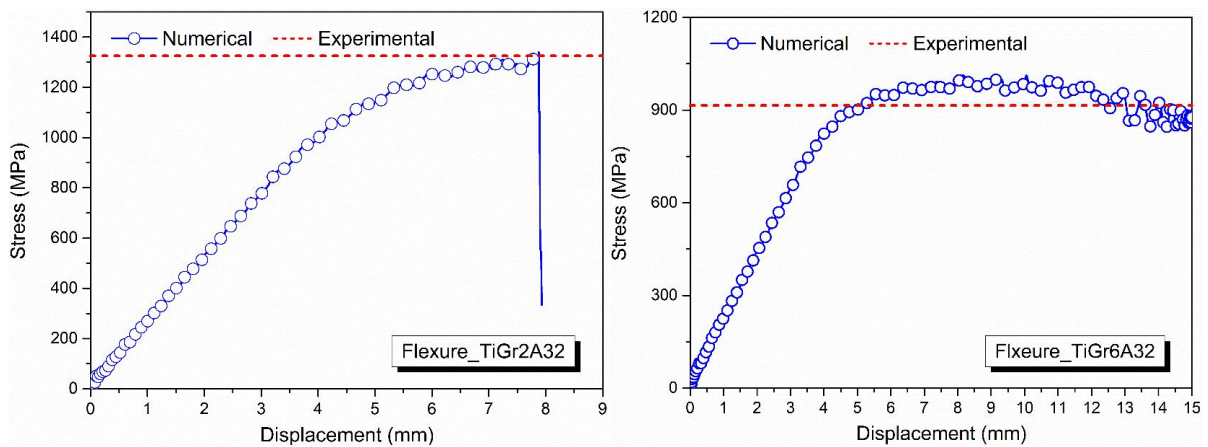


(a) off-axis angle vs shear strength (b) off-axis angle vs off-axis sensibility
 Figure 12: Influence of fiber laying Angle.

Analysis of Bending Strength Calculation Results

Figure 13 shows the flexural load-deflection curves of TiGr2A32 and TiGr6A32 respectively, while Table 8 shows the relative errors of TiGr2A32, TiGr2A43 and TiGr6A32.

It can be seen from the figure and table that the bending model of TiGr can predict the ultimate bending strength more accurately. For TiGr2A structure, when the load reaches its ultimate load, the bending load-deflection curve is greatly reduced instantly, while for TiGr6A structure, when the load exceeds its ultimate strength, the curve shows a slow decline. This difference is mainly related to the different damage modes of the two structures. In addition, by comparison, it can be found that when the CFRP layer is laid in the same way, a slight change in the ratio of titanium alloy layer to CFRP layer will not significantly affect the ultimate bending strength, but when the direction of CFRP layer changes, the bending strength changes significantly.



(a)TiGr2A32 bending load-deflection curve (b)TiGr6A32 bending load-deflection curve
 Figure 13: Bending load - Deflection curve.

Table 8: Bending strength of TiGr.

Type of structure	Experiment (MPa)	Simulation (MPa)	Relative Error (%)
TiGr2A32	1325	1339.99	1.13
TiGr2A43	1247	1320.30	5.88
TiGr6A32	915	1013.20	10.73

The damage modes of titanium alloy layers, CFRP layers and interfacial adhesive film layers in TiGr2A32 structure are shown in Table 9.

Table 9: Bending damage modes of TiGr2A32.

Damage mode	1 ^a	2	3	4
Ti-PEEQ				b
CFRP-FT				
CFRP-FC				
CFRP-MT			c	c
CFRP-MC			c	c
AD-SDEG				

a- number order for top to bottom (top for loading side)

b- Not involved

c- No corresponding form of injury is present

As can be seen from the table, when TiGr is subjected to bending load, the titanium alloy layer far away from the loading side is basically not damaged. For CFRP layer, the compression damage occurs mainly near the loading side, while the tensile damage occurs away from the loading side, which is just in line with the mechanical characteristics of the bending beam. Under such stress characteristics, the upper and lower CFRP layers show obvious fiber compression and fiber tensile damage, respectively. For TiGr2A, the matrix damage of CFRP layer does not show obvious "pressing up and pulling down", while some layers show no matrix damage phenomenon, which is mainly related to the overall failure mode of TiGr2A structure. As can be seen from the figure, the failure of TiGr2A is mainly controlled by the failure of titanium alloy -CFRP interfacial adhesive film.

SUMMARY

In this paper, the static behaviors of TiGr are studied experimentally and theoretically. The conclusions are as follows:

(1) The failure mode of TiGr was normal, and the materials showed mixed characteristics of metal and fiber composites during the test. The stress-strain curves showed yield characteristics during the tensile and shear processes. Due to the low content of carbon fiber in the sample, its failure strength showed a strong correlation with metal. In the future, more studies will be carried out on the properties of titanium alloy hybrid materials with typical layering structures.

(2) By establishing a finite element model, the static behavior of TiGr under tensile, shear, and bending conditions were analyzed. The effectiveness of the established model was verified based on the test results. Combined with the damage analysis of the constituent materials, the damage mechanism, constituent ratio, laying direction and other factors on the mechanical properties are described.

REFERENCES

- [1] S.M.R.Khalili1, V.Daghigh and R.Eslami Farsani. Mechanical behavior of basalt fiber- reinforced and basalt fiber metal laminate composites under tensile and bending loads. *Journal of Reinforced Plastics and Composites* 30(8) 647–659.
- [2] Yury Solyaev, Arseniy Babaytsev. Direct observation of plastic shear strain concentration in the thick GLARE laminates under bending loading. *Composites Part B* 224 (2021) 109145.
- [3] Masoud Haghi Kashani, Mojtaba Sadighi, Melika Mohammadkhah and Hamid Shahsavari Alavijeh. Investigation of scaling effects on fiber metal laminates under tensile and flexural loading. *Proc IMechE Part L:J Materials: Design and Applications* 2015, Vol. 229(3) 189–201.
- [4] Konrad Dadej, Barbara Surowska, Jarosław Bieniaś. Isostrain elastoplastic model for prediction of static strength and fatigue life of fiber metal laminates. *International Journal of Fatigue* 110 (2018) 31–41.
- [5] Huaguan Lia, Yiwei Xu, Xiaoge Hua, Cheng Liu, Jie Tao, Bending failure mechanism and flexural properties of GLARE laminates with different stacking sequences. *Composite Structures* 187 (2018) 354–363.